研究解説

# GaN and Related Compounds for MEMS and MOEMS

Stanislas K. KRAWCZYK*, Takao SOMEYA*, Yasuhiko ARAKAWA* and Hiroyuki FUJITA*

## 1. Introduction.

We are strongly motivated by this work for the following reasons :

1) Outstanding intrinsic properties of GaN and related compounds:[e.g.1,2] :
   In particular, direct and wide band gaps of these materials allow for efficient generation and detection of UV light and ensure excellent chemical stability even at elevated temperatures.
2) Already achieved technological maturity of GaN materials and devices:[e.g..2-4] :
   Blue GaN LEDs are already widely commercialized and violet LDs are entering in the industrial production. Demonstrated micro-electronic devices (HEMTs and HBTs) exhibit excellent high frequency and high power performance.
3) New MEMS and MOEMS for some specific applications and expected break through in UV opto-electronics, which almost does not exist yet:
   In particular, integrated MOEMS for spectroscopic detection of molecules having absorption bands in the UV domain of wavelengths should be of interest for bio-chemical, pharmaceutical, automotive and space industries as well as for environmental control applications (e.g. ozone detection).

## 2. Demonstrator devices.

The detailed aims of this project are to build-up few demonstrator devices exploring both vertical and planar active/passive UV GaN optical components integrated with mechanical components. These include the following MOEMS:

1) Tunable light sources and detectors for UV spectroscopy and high temperature operation based on GaN photo-detectors, LEDs and VCSELs integrated with electrically controlled vertical air-gap Fabry-Perot optical filters.
2) Pressure, acceleration and vibration sensors, which make use of active GaN optoelectronic devices, planar GaN optical guides and Mach-Zehnder interferometers located over a membrane or close to a cantilever.

*3 rd Department, Institute of Industrial Science, University of Tokyo

## 3. GaN-based tunable light sources and detectors for UV spectroscopy and high temperature operation.

### 3.1. Principle.

The GaN-based tunable light sources and detectors for UV spectroscopy and high temperature operation include (Fig.1) :

An active component (photo-detector, LED or VCSEL) implemented on the GaN layer deposited by MOCVD on the sapphire substrate.

An electrically tunable vertical resonant Fabry-Perot cavity, which is formed by an air-gap and a movable membrane suspended over the active component. This part of the micro-systems is fabricated using Si compatible materials and technologies, including surface micromachining.

The voltage applied between the bottom cavity region and the electrode incorporated into the membrane induces an electrostatic

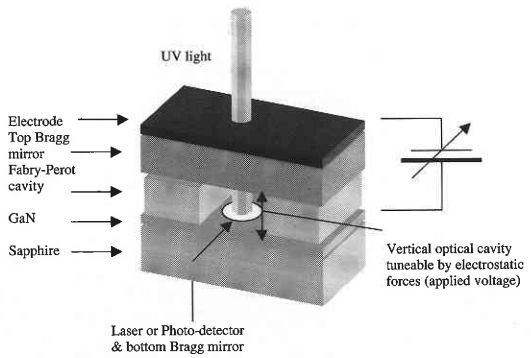


Fig. 1　Principle of GaN-based tunable light sources and detectors for UV spectroscopy and high temperature operation.

force, which reduces the thickness of the air gap. Thus, the resonant frequency of the cavity is modified and the reception and/or emission spectra of the whole device can be "scanned" by changing the applied voltage.

### 3.2. Geometry and principal technological aspects.

A schematic diagram of the overall geometry of our micro-systems is shown in Fig. 2. Four flexible legs attached to four support posts hold the membrane. We deliberately choose a four-legs configuration, as opposed to two legs or cantilever approach, in order to keep the top mirror parallel to the bottom. The most general technological aspects of this structure are presented in Fig. 3.

The bottom and top mirrors of the Fabry-Perot cavity contain Bragg reflectors composed from a sequence of $SiO_2/Si_3N_4$ layers. In addition, the top mirror (membrane) contains a conductive layer. We consider a very thin gold layer (about 10nm thick) or an extremely thin "adhesive" titanium layer followed by this gold layer. The sacrificial layer is made from poly-Si and removed by selective etching.

### 3.3. Optical modeling and design.

Optical simulations were carried out using the dedicated software developed at LIMMS -IIS under MATLAB environment.

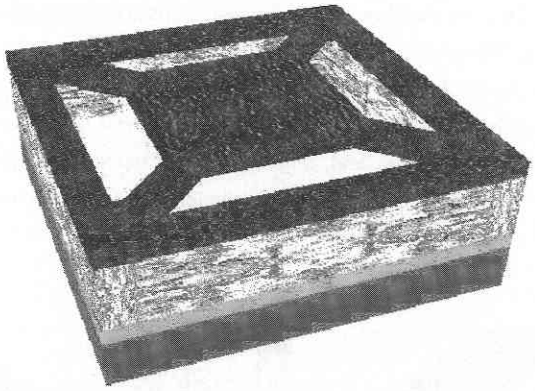

Fig. 2　Geometry of tunable light sources and detectors for UV spectroscopy and high temperature operation.

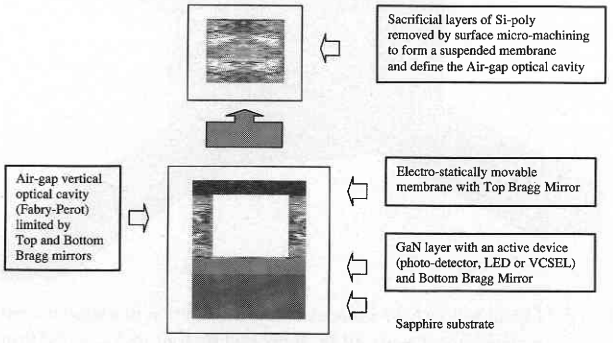


Fig. 3　Illustration of the most general technological aspects.

This software permits:

1) a complete modeling of any multi-layer structure by transfer matrix method (e.g. reflectance and transmittance simulation of the complete Fabry-Perot cavity with top and button mirrors composed from DBR reflectors);
2) to isolate a layer or a combination of several layers (e.g. individual DBR reflector) and to examine the influence of these layers, and of any changes in them, on the performance of the structure as a whole;
3) to calculate the principal optical parameters of the structure, such as mode separation (FSR), full width at half maximum (FWHM), finesse (FSR/FWHM) and contrast.

The simplest configuration of the layers, which ensures both, the adequate optical performance and process simplicity, in the case of photo-detectors, is shown in Fig. 4. The chosen cavity length is 1$\mu$m and the reflectors are designed for the maximum transmittance at wavelengths close to 0.4$\mu$m. The optical transfer functions of this cavity are presented in Fig.5. We found that without the gold layer in the membrane, the total transmittance of the cavity is 99.85 %, FWHM is 5.5nm and the mode separation is of about 30nm. A possible solution that allows compensating the phase shift introduced by the presence of gold, is the deposition of a supplementary $Si_3N_4$ layer on the top of the membrane. Furthermore, this shift can be compensated if the Bragg reflectors contain $SiO_2/Si_3N_4$ layers slightly thicker than 1/4 of the central wavelength. The transmittance of the structure with a gold layer is 80% and FWHM is 6nm.

The results of simulation show that, theoretically, it is not a major problem to improve further the optical properties of the cavity. This can by done by increasing the number of the $SiO_2/Si_3N_4$ pairs in the Bragg reflectors and verifying that the reflectivity of both mirrors are not only as high as possible but also as equal as possible. Another possible solution is to define an optical window (without the metal layer) in the center of the membrane. The key problem, however, is to achieve a good control of the thickness of the deposited layers.

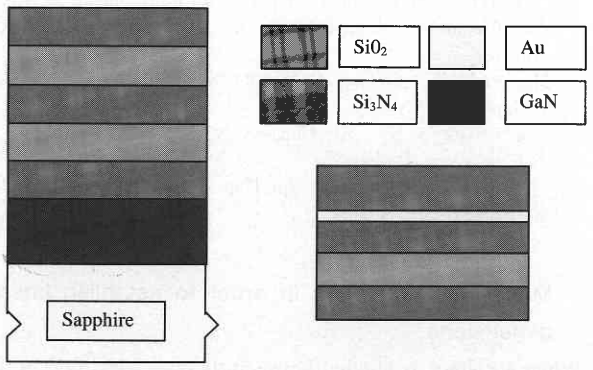


Fig. 4　Schematic presentation of (a) the bottom and (b) the top mirrors.

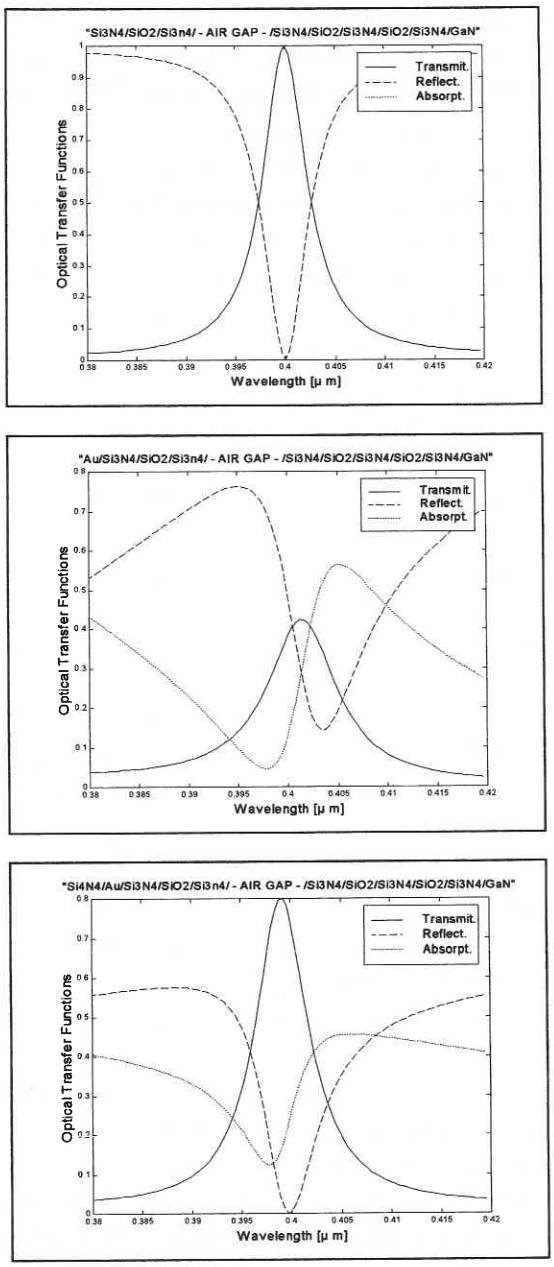


Fig. 5　Examples of optical functions of structures with air cavity length of 1_m, designed for maximum transmittance at wavelengths close to 400 nm but with various configurations of the top mirror:
(a) $Si_3N_4/SiO_2/Si_3N_4$ - Air Gap - $Si_3N_4/SiO_2/Si_3N_4/SiO_2/Si_3N_4$/GaN (no metal layer),
(b) Au/$Si_3N_4/SiO_2/Si_3N_4$ - Air Gap - $Si_3N_4/SiO_2/Si_3N_4/SiO_2/Si_3N_4$/GaN,
(c) $Si_3N_4$/Au/$Si_3N_4/SiO_2/Si_3N_4$ - Air Gap - $Si_3N_4/SiO_2/Si_3N_4/SiO_2/Si_3N_4$/GaN.

### 3.4. Mechanical modeling in order to establish lateral dimensions.

When a voltage is applied between the gold electrode in the membrane and the bottom cavity region, the membrane is electrostatically attracted toward the substrate, reducing the thickness of the air gap cavity. The elastic restoring force of the membrane legs balances the electrostatic force. There is almost a parabolic relationship between the membrane vertical displacement and the applied voltage. However, the maximum air gap change is roughly a third of the initial air gap thickness. For a larger bias, the electrostatic force is always greater than the elastic restoring force of the membrane legs and the membrane is pulled into contact with the substrate. The electrostatic force depends on the surface of the membrane, on the air gap thickness and on the applied voltage. The elastic restoring force is a function of the width, length and the effective spring constant of the membrane legs.

We performed mechanical simulation of the basic structure (described in previous sections) in order to evaluate the optimal lateral dimensions of the membrane and of the legs. The objective is to attain a large tuning range with low applied voltage and do not exceed the maximum fracture stress during device operation. We also evaluated the frequency response of the structure. The simulation was carried out using ANSYS model. We analyzed a large number of possible lateral dimensions of the membrane and the legs. The results presented in Fig.6 appear particularly interesting.

Thus, he membrane with dimension 30$\mu$mx30$\mu$m supported by legs 25$\mu$mx10$\mu$m seems to be adapted for our application. The applied voltage of 10V results in a vertical displacement of the membrane close to 0.25$\mu$m. This displacement is still lower that the critical value and causes the shift of the wavelength of 100nm. The maximum strain in the legs appears to be lower that the expected maximum fraction strain for this type of materials.

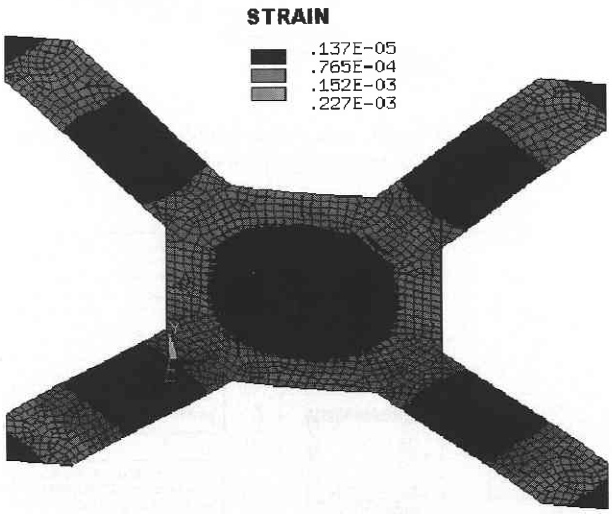


Fig. 6　Calculated (ANSYS model) strain distribution in a structure with a membrane 30$\mu$mx30$\mu$m, supported by four legs 25$\mu$mx10$\mu$m; cavity length 1$\mu$m; bias 10 V.

The first resonant frequency is at 283 kHz and indicates that the maximum modulation frequency should be above 250kHz.

The results obtained, although very promising, provide only an estimation of a reasonable range of lateral dimensions of the structure and of the expected performances. In fact, the real mechanical properties of the deposited layers are strongly process dependent and can be only established experimentally on the completed test structures. However, the above analysis is indispensable for the mask design and for process optimization.

### 3.5. Process tolerance.

It should be noted that the sputtering or CVD deposition of dielectric layers as well as electron beam deposition of the gold film couldn't be as well controlled as the epitaxial growth (thickness and refractive index). We evaluated the effect of a possible inaccuracy in the thickness control of different layers on the spectral transmittance of our structures. The results obtained with the previously discussed structure are shown in Fig 7.

## 4. Conclusions.

Although successful association of photo-detectors or VCSELs with tunable air-gap Fabry-Perot cavity was already demonstrated for other wavelengths and semiconductors [5-7], we can only partially use the existing expertise in that field. In fact, the choice of UV-transparent materials compatible with the Si-technology is limited, we must introduce a metal layer into the top mirror and even the complex refractive index of $Si_3N_4$ changes drastically in the UV domain. In addition, short wavelengths (200nm - 400nm) demand sever compromises between the dimensions of the structure and process limitations (micromachining)

Thus, an appropriate software package for optical design and simulation of MOEMS with an optical cavity has been developed (transfer matrix method). It allows analyzing any type of vertical structures. Several basic configurations of tunable light sources and detectors for UV spectroscopy have been designed. Optical, electrical and mechanical aspects were taken into consideration, which allowed defining a family of test structures with reasonable dimensions and reasonably good expected characteristics. For example in the case of tunable photo-detectors, we can expect a tuning range up to 100nm, with a bias voltage of 10V, and a spectral selectivity below 5nm. This structure could potentially work up to modulation frequencies close to 250kHz.

We limited our presentation here to the simplest solutions, which will be used for optimization of processing steps and first experimental validations of our concepts in the case of photodetector based microsystems. On the other hand, the simulation results show that it is still possible to improve, the optical properties of the cavity thanks to additional $SiO_2/Si_3N_4$ layers, by introducing air-gaps inside the Bragg reflectors or an optical window in the metal layer in the membrane.

However, the main question now, is to achieve a good control of the quality and of the reproducibility of the processing steps. Then, the key performance goals will be (i) wavelength selectivity, (ii) wide tuning range, (iii) high sensitivity and (iv) high temperature operation in chemically hostile environments.

(Manuscript received, June 28, 1999)

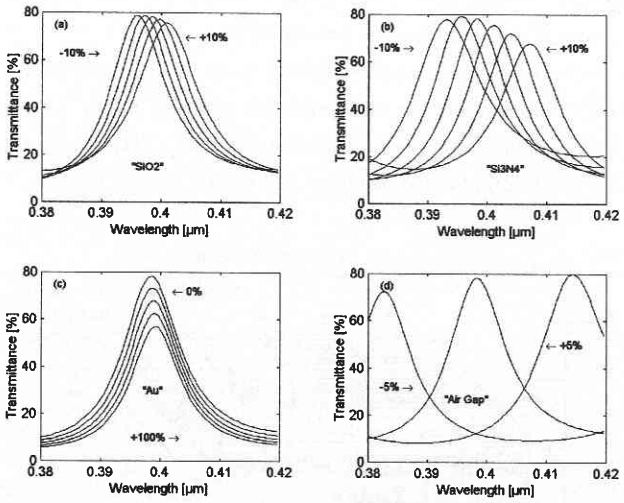


Fig. 7 Effect of the thickness inaccuracy of $SiO_2$, $Si_3N_4$, Au and of the sacrificial poly-Si layers on the spectral transmittance of the structure: $Si_3N_4/Au/Si_3N_4/SiO_2/Si_3N_4$ - Air Gap - $Si_3N_4/SiO_2/Si_3N_4/SiO_2/Si_3N_4/GaN$. The increment of the error between the minimum and the maximum value is equal and specific for each diagram.

### Reference


1) S. Strite and H. Morkoc, "GaN, AlN, InN : A review", J. Vac. Sci. Tech., B 10(4), 1237, 1992.
2) H. Morkoc, S. Strite, G.B. Gao, M.E. Lin, B. Sverdlow and M. Burns, "Large-band-gap SiC, III-V nitrides, II-VI ZnSe-based semiconductor technologies", J. Appl. Phys., 76(3), 1363, 1994.
3) I. Akasaki and H. Amano, "Crystal growth and conductivity control of Group III nitride semiconductors and their application to short wavelength light emitters", Jpn. J. Appl. Phys., 36, 5393, 1997.
4) S. Nakamura and G. Fasol, "The Blue Laser Diode", Springer, Berlin, 1997.
5) C. Seassal, J.L. Leclercq and P. Viktorovitch, "Fabrication of InP based free standing microstructures by selective surface micromachining" J. Micromach. Microeng., 6, 261, 1996.
6) F. Sugihwo, M.C. Larson, "Micromachined widely tunable vertical cavity laser diodes", J. of Microelectromechanical Systems, 7, 1, 1998.
7) M.Y. Li, W. Yuen, G.S. Li, C.J. Chang-Hasnain, "Top-emitting micromechanical VCSEL with a 31.6. tuning range", IEEE Photonics Tech. Lett., 10, 18, 1998.